Trapping of trace gases in growing ice crystals

B. Kärcher

Institut für Physik der Atmosphäre (IPA), Deutsches Zentrum für Luft- und Raumfahrt Oberpfaffenhofen, Wessling, Germany

M. M. Basko

Institute for Experimental and Theoretical Physics (ITEP), Moscow, Russia

Received 20 July 2004; revised 16 September 2004; accepted 23 September 2004; published 20 November 2004.

[1] An analytical model describing the combined effect of mass accomodation and net adsorption of trace gases on the surfaces of growing ice particles (trapping) is developed. An approximate solution for the release of trapped trace gases from evaporating ice particles is also given. The model fully accounts for the fact that atmospheric ice particles frequently experience substantial subsaturations and supersaturations. In such situations, pure adsorption models cannot be employed to calculate the trace gas uptake. Limiting cases are discussed in which uptake is solely controlled by gas diffusion (burial limit) or by surface kinetics (adsorption limit). The model results are expressed in terms of a nonreactive uptake coefficient for use in atmospheric models. Crucial factors controlling trapping are the rate of desorption (or net molecular escape rate) and the ice growth rate. Trace gase molecules can be effectively trapped in bulk ice even at low ice supersaturations when their times of adsorption are sufficiently long. The trapping model may help provide physically sound interpretations of field and laboratory measurements of trace gas uptake on growing ice surfaces. Previous global model studies of nitric acid uptake in cirrus clouds only considering adsorption likely underestimated the resulting dentrification, because the vertical redistribution is driven by the largest ice crystals which trap nitric acid most efficiently. *INDEX TERMS:* 0305 Atmospheric Composition and Structure: Aerosols and particles (0345, 4801); 0320 Atmospheric Composition and Structure: Cloud physics and chemistry; 0365 Atmospheric Composition and Structure: Troposphere—composition and chemistry; 0322 Atmospheric Composition and Structure: Constituent sources and sinks; *KEYWORDS:* trace gases, ice crystals, trapping

Citation: Kärcher, B., and M. M. Basko (2004), Trapping of trace gases in growing ice crystals, *J. Geophys. Res.*, *109*, D22204, doi:10.1029/2004JD005254.

1. Introduction

[2] The understanding of the physical processes governing uptake and incorporation of trace gases in ice crystals and snowflakes is crucial for quantifying the effects of heterogeneous chemistry in the present and future climate [*World Meteorological Organization* (*WMO*), 2003] and the chemical composition of polar ice cores used to reconstruct our past climate [*Legrand*, 1994].

[3] The term trapping refers to the irreversible, nonreactive uptake of trace gases on solid particles which grow due to an external forcing. More specifically, in this work, trapping refers to the combined effect of mass accomodation and desorption of molecules at an ice crystal surface that grows from the vapor phase by the deposition of water (H_2O) molecules.

[4] Previous theoretical studies have examined the interaction of trace gases with ice particles by means of surface adsorption models [e.g., *Tabazadeh et al.*, 1999; *Carslaw and Peter*, 1997]. While this may be adequate to study the interaction with nongrowing surfaces in thermodynamic equilibrium conditions, pure adsorption models are incapable of adequately describing the considerable variability in observed nitric acid (HNO_3) content in cirrus ice crystals [*Popp et al.*, 2004].

[5] Adsorption models do not consider that atmospheric ice crystals frequently grow and evaporate during the lifecycle of clouds. A plethora aircraft and remote sensing measurements reveal that cloud elements evolve in a highly dynamic environment. Fluctuations of temperature on various spatial and temporal scales cause the frequent occurrence of subsaturations and supersaturations, and hence the ice particles are hardly found in steady state conditions over an extended period of time. Here, we develop and examine for the first time an analytical model that fully accounts for the fact that gas-ice interactions take place in a dynamic, non-steady-state ambient environment.

[6] We suggest that gas phase diffusion of trace gas molecules toward growing ice crystals in addition to surface kinetics is a prerequisite for a proper description

0148-0227/04/2004JD005254

of uptake. We show that the effects of trapping can be expressed in terms of a nonreactive uptake coefficient that depends on the temperature, ice particle size and radial growth rate, and the gas diffusion coefficient, sticking probability, and rate of desorption of trace gas molecules. Diffusion of the trace gas into the ice phase is not important for trapping on the timescales of interest. We delineate limiting cases where trapping is solely controlled by gas diffusion (burial limit) or by surface kinetics (adsorption limit). We also propose a method to treat the release of the trace gas along with H_2O from evaporating ice crystals.

[7] The analytical model is described and examined in sections 2 and 3. Applications of the results in a detailed numerical process model are presented in section 4. A discussion of uncertainties and the conclusions are given in sections 5 and 6, respectively. Appendices A, B, and C focus on an estimate of the diffusion of molecules into bulk ice, a modification of the model to describe trapping on growing ice films in free molecular flow, and the numerical solution of the model equations, respectively.

2. Model

2.1. Ice Crystal Growth

[8] If the air is supersaturated with respect to the ice phase, ice crystals will grow by deposition of H_2O (subscript w) molecules at their surfaces. Air temperature T and pressure P are given and are not affected by crystal growth or evaporation, and differences between particle and air temperature can be ignored in cirrus or polar stratospheric cloud conditions (185 K < T < 235 K). The diffusional growth law for spherical ice particles with radius a can be written as [*Pruppacher and Klett*, 1997]

$$\dot{a} \equiv \frac{da}{dt} = \nu_w \frac{D_w \beta_w}{a} \frac{p_i}{k_B T}(S_i - \delta), \quad \beta_w = \left(1 + \frac{4D_w}{\alpha_w u_w a}\right)^{-1} \tag{1}$$

with the volume ν_w of H_2O molecules in ice, the diffusion coefficient $D_w(P, T)$ of H_2O molecules in air, Boltzmann's constant k_B, the ice saturation ratio S_i, the saturation vapor pressure over ice $p_i(T)$, and the Kelvin term δ accounting for the enhancement of p_i over small crystals. The function $\beta_w(a)$ interpolates between the kinetic ($a\alpha_w \gg 4D_w/u_w$) and the diffusion ($a\alpha_w \ll 4D_w/u_w$) limit, where α_w is the deposition coefficient of H_2O molecules on ice and $u_w = \sqrt{8k_BT/(\pi m_w)}$ is their mean thermal speed. Finally, in u_w, m_w denotes the mass of an H_2O molecule.

[9] For simplicity, we omit in equation (1) ventilation effects that become important for large (a > 50 μm) crystals, latent heat effects ($\propto p_i$) that become important for T > 235 K, and shape corrections accounting for a possible nonspherical habit of ice crystals, in which case a denotes the radius of a volume-equivalent sphere. All of these effects are straightforward to implement in equation (1).

[10] The above expression for β_w holds under the assumption that all molecules leaving the ice surface are instantaneously thermalized. In reality, the molecules first have to travel a distance of the order of one mean free path ($3D_w/u_w$) in order to collide with air molecules and thermalize. The correct form of β including this effect differs only slightly from equation (1).

2.2. Trace Gas Trapping

[11] Trace species may deposit on the surfaces of ice crystals, besides H_2O. The number of molecules taken up by gas diffusion per unit time is given by

$$\frac{dN}{dt} = 4\pi a D \beta n_\infty \geq 0, \quad \beta = \left(1 + \frac{4D}{\alpha u a}\right)^{-1}, \tag{2}$$

where n_∞ is the trace gas concentration far away from the ice particle. As for equation (1), this expression may easily be extended to include the effects of ventilation and crystal shape, while the latent heat correction is negligible owing to the low trace gas concentrations.

[12] If the air above the ice particle is exactly at saturation (a = *const.*), an adsorption equilibrium establishes between the trace gas and the ice particle surfaces, as discussed in section 2.3. If the ice particles evaporate, the trace gas will leave the ice particles along with H_2O. If the ice particles grow, trace gas molecules may become trapped by deposition of many ice layers. Trapping is irreversible as long as $S_i > \delta$. This work investigates the trapping process in more detail and extends equation (2) to include this effect.

[13] The efficiency of trapping depends on the probability of the trace gas molecules to accomodate at the surface and on the probability to desorb, or in more general terms, escape from the surface, after successful uptake. Further, the trapping efficiency must depend on the radial growth rate $\dot{a} > 0$ of the ice crystals. We argue later in section 2.4 that diffusion of gas molecules into the ice phase is unimportant for ice crystal growth under atmospheric conditions.

[14] While for rapidly growing ice crystals, all available trace gas molecules will be buried in the bulk of the ice, the trapping efficiency will decrease and approach the pure adsorption limit as $\dot{a} \to 0$. The dimensionless parameter

$$\kappa = \frac{D}{a\dot{a}} \tag{3}$$

represents the ratio of the "gas diffusion velocity" D/a and the velocity $\dot{a}$ of the phase boundary. Alternatively, it can be viewed as the ratio of the growth timescale $a/\dot{a}$ and the gas diffusion timescale a^2/D.

2.3. Surface Kinetics

[15] Before we set up and solve the model equations, we examine the kinetics of adsorption and desorption of molecules at the ice surface in more detail. We use this information to define the boundary condition for our problem in section 2.5.

[16] We use the subscripts + and − to denote gas phase and ice phase at the phase boundary (i.e., at the radial position $r = a$), respectively. The number of molecules adsorbing at the surface from the gas phase per unit surface area and per unit time is given by $n_+ \cdot \alpha_+ u/4$, with the mass accomodation (or deposition, condensation) coefficient α_+. The number of molecules leaving the ice surface (in the same units) can be cast into the form $n_- d \cdot k$, with the first order desorption rate $k(T)$ and the surface depth d.

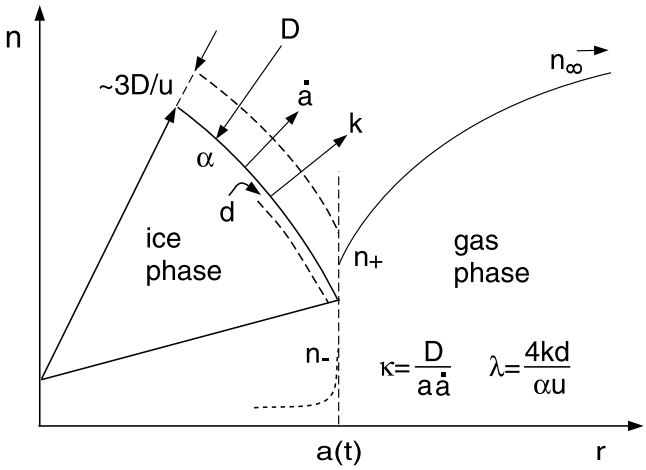

Figure 1. Schematic of processes associated with the trapping of trace gas molecules by growing ice particles. The coordinate axes refer to the radial number density profile of the molecules, while the spherical segment illustrates the processes occurring at the gas-ice interfacial boundary. The gas profile inside ice is plotted as a dotted curve to indicate that diffusion in ice is negligible over the timescales of interest. The solution $n(r \geq a)$ quickly assumes a quasi-steady-state upon changes in a.

[17] The term $n_{-}d$ can be viewed as a depth-integrated number of molecules per cm^2 of ice particle surface area. The surface concentration $n_{-}d$ is equivalent to θ/σ, where θ is the fractional surface coverage and σ is the surface area per available adsorption site. As $\theta = 1$ is equivalent to $n_{-}^{\max} = 1/(\sigma d)$, we identify σd as the volume per adsorption site, hence d as the average thickness of a (partial) molecular layer adsorbed at the ice surface.

[18] The desorption rate can be written as $k = \alpha_{-}\omega\exp[-Q/(k_B T)]$, with the evaporation coefficient α_{-}, the frequency ω of oscillations of adsorbed molecules perpendicular to the surface, and the heat of adsorption $Q > 0$ [*de Boer*, 1968]. Its inverse, $1/k$, is the time of adsorption of the trace gas molecules at the ice surface. We will assume $\alpha_{+} = \alpha_{-} = \alpha$ throughout this work.

[19] The dimensionless parameter

$$\lambda = \frac{4kd}{\alpha u} \tag{4}$$

measures the desorption flux relative to the adsorption flux. Rewriting the equilibrium relation $n_{+}\alpha u/4 = n_{-}kd$ allows us to relate λ to the equilibrium constant $K(T)$ for adsorption,

$$\theta = Kp_{+}, \quad K = \frac{\sigma d}{k_B T}\frac{1}{\lambda} = \frac{\sigma u/\omega}{4k_B T}\exp\left(\frac{Q}{k_B T}\right), \tag{5}$$

where $p_{+} = n_{+}k_B T$. Note that α cancels out in equations (4) and (5). We note that the value of Q may depend on T as the nature of the ice surface changes with T, and the exponential prefactor of k is only an upper limit value valid for mobile adsorption. These values may be adjusted for specific molecules once they have been validated for ice surfaces.

[20] We are fully aware of the fact that the first order desorption rate introduced here may not always be adequate to describe the surface kinetics. However, it is a convenient tool the examine the relative roles of the different processes and timescales controlling trapping in a first approach. If other processes influence the time the molecules spend on the ice surface, we suggest here to view k as an effective molecular escape rate, see also section 2.4. Modifications of k in this sense are further discussed in section 5.4.

2.4. Basic Model Assumptions

[21] Our model is based on two key assumptions.

[22] 1. Diffusion of trace gas molecules toward the ice particle surface ($r > a$) can be approximated by a steady state profile.

[23] The timescale over which gas phase diffusion comes into steady state is given by a^2/D. As D is of the order 0.1–1 cm^2 s^{-1}, even for large ice crystals with $a = 100$ μm, this timescale is in the range 0.1–1 ms.

[24] Ambient variables such as a, T, and n_∞ change over much longer timescales. For instance, the timescale $a/\dot{a}$ of radial growth from equation (1) is >1 min for $T < 235$ K and $S_i - \delta = 0.1$, increasing exponentially when T decreases. Hence assumption 1 leads to $\kappa \gg 1$, valid for any value $\dot{a} \geq 0$. It is easy to verify that this condition holds at all T below the melting point of ice. The gas diffusion timescale also applies to situations where the steady state concentration profile is not spatially uniform.

[25] 2. Diffusion of trace gas molecules into the ice particles ($r < a$) can be neglected.

[26] The timescale for molecular diffusion within bulk ice is given by a^2/D_i. Here, D_i decreases exponentially with decreasing T and is typically below 5×10^{-13} cm^2 s^{-1} at $T <$ 235 K. This value holds for self-diffusion of H_2O in ice [*Pruppacher and Klett*, 1997] and may serve to roughly approximate the order of magnitude of D_i for other molecules as well. Hence, even for small ice crystals with $a =$ 10 μm, this timescale is >550 h.

[27] If we opted to include ice phase diffusion, a steady state approximation would only be justified if $D_i \ll a\dot{a}$ (see Appendix A); other cases, in particular the case $\dot{a} = 0$, would require a non-steady-state solution. However, because the timescale a^2/D_i is so much longer than $a/\dot{a}$, we may ignore molecular diffusion within ice. Assumption 2 implies that uptake is confined to an infinitely thin surface layer.

[28] Our model does not resolve all processes that may take place in the real surface layer. One example may be rapid diffusion into a disordered surface layer of water. However, we think that such modifications do not invalidate our trapping model and could be incorporated into an effective escape rate instead of using the simple desorption rate from section 2.3. More details are presented in section 5. The physics of trapping outlined above is summarized in Figure 1.

2.5. Trapping Equations and Solution

[29] Following assumption 1, the steady state flux at the phase boundary $r = a$ of molecules diffusing in air toward a spherical particle is given by $(n_{+} - n_\infty)D/a$ [*Crank*, 1956], where $n_\infty = n(r \gg a)$.

[30] In a reference frame moving with the velocity $\dot{a} > 0$ in the direction of increasing r, the total flux f at $r = a$ is the sum of the advective flux, $-n\dot{a}$, and the diffusion flux:

$$f_+ = -n_+\dot{a} + (n_+ - n_\infty)D/a, \tag{6a}$$

$$f_- = -n_-\dot{a}, \tag{6b}$$

where we ignored diffusion into the ice particle (assumption 2). The boundary condition describing net adsorption of molecules at a boundary moving with velocity $\dot{a} > 0$ is given by

$$f_b = -n_+\dot{a} + (\lambda n_- - n_+)\alpha u/4, \tag{6c}$$

where we use the adsorption model introduced in section 2.3.

[31] The fluxes (6a), (6b), and (6c) must be continuous at the phase boundary:

$$f_- = f_+ = f_b, \tag{7}$$

constituting a set of two algebraic equations for the two unknowns n_+ and n_-, the solution of which is given by

$$\frac{n_+}{n_\infty} = (1-\beta) + \beta\lambda\frac{n_-}{n_\infty} \tag{8a}$$

$$\frac{n_-}{n_\infty} = \frac{1+\beta(\kappa-1)}{1+\beta(\kappa-1)\lambda}. \tag{8b}$$

In the limit $\beta(\kappa - 1)\lambda \gg 1$, we find $n_- \to n_\infty/\lambda$, representing the full equilibrium solution with zero net adsorption and vanishing total flux, i.e., $n_\infty = n_+ = \lambda n_-$ and thus $\dot{a} = 0$.

[32] We recall that equation (8b) is only valid for $\kappa \gg 1$, otherwise the steady state assumption breaks down. Hence our final practical solution reads

$$\frac{n_-}{n_\infty} \xrightarrow{\kappa\gg 1} \frac{1+\beta\kappa}{1+\beta\kappa\lambda}. \tag{9}$$

The net number of trace gas molecules trapped per ice particle per unit time is given by

$$\frac{dN}{dt} = 4\pi a^2 n_-\dot{a}. \tag{10}$$

Inserting the asymptotic expression (9), the final solution reads

$$\frac{dN}{dt} = 4\pi a D n_\infty \varepsilon, \quad \varepsilon = \frac{\beta + 1/\kappa}{1+\beta\kappa\lambda}, \tag{11}$$

where we have defined the dimensionless trapping efficiency ε, which describes the transition from adsorption to burial and replaces β in equation (2).

[33] Uptake coefficients are widely used in atmospheric heterogeneous chemistry. They enable the combined effects of gas and liquid phase diffusion, solubility, and chemical reaction in liquid aerosol particles to be described in the framework of the gas diffusion rates of the reactant molecules. Here we develop a similar concept to describe the nonreactive trapping of trace gases in growing ice particles.

[34] The uptake coefficient γ is defined as the overall net flux of molecules into the ice particle divided by the (maximum) kinetic collision flux at $r = a$,

$$\gamma = \frac{n_-\dot{a}}{n_+ u/4}. \tag{12}$$

Inserting equation (9) and using again $\kappa \gg 1$, it is easy to show that γ takes the form

$$\frac{\alpha}{\gamma} = \frac{\beta}{1-\beta}\left(\frac{1}{\varepsilon} - 1\right), \tag{13}$$

with the trapping efficiency defined in equation (11). By comparing equations (11) and (13) we see that ε and γ are related via

$$\varepsilon = \left(1 + \frac{4D}{\gamma u a}\right)^{-1}. \tag{14}$$

We note in passing that γ is identical to the burial coefficient defined by *Yin et al.* [2002].

[35] Equations (11) and (13) have the following limiting cases.

[36] 1. $\beta\kappa\lambda \ll 1 \Rightarrow \varepsilon \to \beta + 1/\kappa$ (burial limit). Diffusion or ice particle growth are fast and desorption plays no role in trapping; i.e., the net uptake does not depend on λ.

[37] In the case $\beta\kappa \gg 1$, we find

$$\varepsilon = \beta, \quad \gamma = \alpha, \quad \frac{dN}{dt} = 4\pi a D \beta n_\infty; \tag{15a}$$

this represents diffusion-limited burial, which maximizes when $\beta \to 1$. If $\beta \ll 1$ because the impinging molecules do not accomodate efficiently and/or the ice particles are very small, we obtain kinetically-limited burial from equation (15a):

$$\frac{dN}{dt} = 4\pi a^2 n_\infty \frac{\alpha u}{4}.$$

[38] In the case $\beta\kappa \ll 1$, we find

$$\varepsilon = \frac{1}{\kappa}, \quad \frac{\gamma}{\alpha} = \frac{1-\beta}{\beta}\frac{1}{\kappa}, \quad \frac{dN}{dt} = 4\pi a^2 n_\infty \dot{a}; \tag{15b}$$

this represents ice particle growth-dominated burial.

[39] 2. $\beta\kappa\lambda \gg 1 \Rightarrow \varepsilon \to [1 + 1/(\beta\kappa)]/(\kappa\lambda)$ (adsorption limit). Diffusion or ice particle growth are slow so that trapping is controlled by the surface kinetics and uptake is dominated by the rate of desorption.

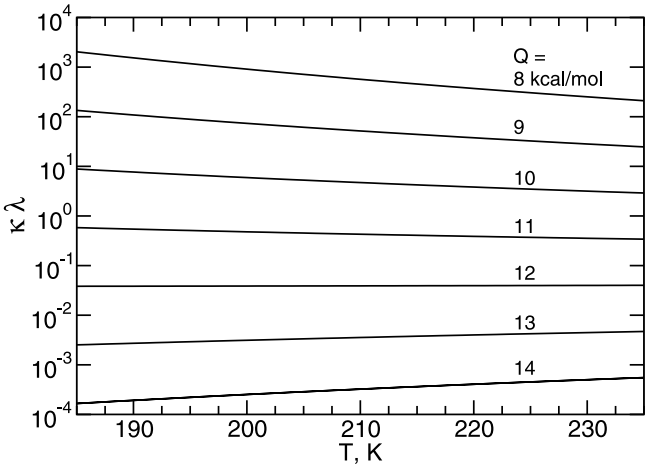

Figure 2. Product $\kappa\lambda$ versus temperature T evaluated for typical microphysical parameters, including $a = 10$ μm and $S_i - \delta = 0.05$ (see text for details). The numbers on each curve denote the assumed heat of adsorption.

[40] In the case $\beta\kappa \gg 1$, we find

$$\varepsilon = \frac{1}{\kappa\lambda}, \quad \frac{\gamma}{\alpha} = \frac{1-\beta}{\beta}\frac{1}{\kappa\lambda}, \quad \frac{dN}{dt} = 4\pi a^2 \frac{n_\infty}{\lambda}\dot{a}. \tag{15c}$$

[41] In the case $\beta\kappa \ll 1$, we find

$$\varepsilon = \frac{1}{\beta\kappa^2\lambda}, \quad \frac{\gamma}{\alpha} = \frac{1-\beta}{\beta}\frac{1}{\beta\kappa^2\lambda}, \quad \frac{dN}{dt} = 4\pi a^2 \frac{n_\infty}{\beta\kappa\lambda}\dot{a}. \tag{15d}$$

Note that $\varepsilon \ll \beta$ in equation (15c) and $\varepsilon \ll 1/\kappa$ in equation (15d).

[42] The molar ratio $\mu = N/N_w$ of trace gas and H_2O molecules in ice is given by $\mu = (dN/dt)/(dN_w/dt)$, where $dN_w/dt = 4\pi a^2\dot{a}/\nu_w > 0$ is the deposition rate of H_2O molecules that follows from equation (1).

[43] In Appendix B we provide a solution to the same problem in planar geometry for molecules moving in free molecular flow. Such a model may be adequate, perhaps with suitable modifications, to describe nonreactive uptake in Knudsen cell experiments.

2.6. Solution for Evaporating Ice Crystals

[44] Upon evaporation of H_2O molecules in subsaturated ambient air ($S_i < 1$), the trapped gas molecules may coevaporate and reenter the gas phase. In principle, equation (11) allows us to track the radial distribution of trapped molecules as a function of time, if the adsorbed molecules become truly buried, and this distribution could form the basis for a solution describing the release of trace gases. However, a steady state solution similar to what we have derived above for trapping is not possible in this case.

[45] We identify two reasons for the failure of a steady state ansatz. First, let us assume, for illustration, that the trace gas is uniformly distributed within the ice particle. Then, even a very small value of D_i will change n_- significantly over a small depth close to the ice surface compared to the remaining concentration $n(r < a)$. Second, a limited number of trace gas molecules evaporating from a thin surface shell is clearly unable to instantaneously control the entire distribution $n(r > a)$ up to n_∞.

[46] One way to proceed would be to seek a time-dependent solution of the evaporation problem, which, however, would lack the desired simplicity for applications of our model. Another aspect is that most atmospheric models are not designed to compute and store the radial distribution of gases in ice particles, so this information would not be available for accurate computations of trace gas release.

[47] Therefore we propose that it may be sufficient to approximate

$$\frac{dN}{dt} = \mu\frac{dN_w}{dt} \tag{16}$$

during ice evaporation, where $dN_w/dt < 0$ is the evaporation rate of H_2O molecules.

[48] Equation (16) essentially assumes a uniform mixing ratio $\mu = N/N_w$ in the ice at any instant. While this may not always be appropriate for tracking the individual temporal history of N for a single ice crystal, we believe that this approach is suitable for any statistical evaluation of the trace gas partitioning averaged over the life cycle of one ore more ice clouds. Such statistical analyses are suitable for comparisons with field observations of gas-ice interactions.

3. Analysis of Model Results

[49] Using the ice vapor pressure $p_i = p_0\exp[-L/(k_BT)]$ with $p_0 = 3.445 \times 10^{10}$ mb and the heat of sublimation $L = 12.2$ kcal/mol [*Marti and Mauersberger*, 1993] and combining equations (3) and (4), we find the following scaling of the product $\kappa\lambda$ with T:

$$\kappa\lambda = \frac{1-\beta}{\beta}\frac{kd}{\dot{a}} \propto T^c \exp[-(Q-L)/(k_BT)]. \tag{17}$$

We evaluate this expression for $P = 200$ mb, $a = 10$ μm, $S_i - \delta = 0.05$, and $\alpha_w = 0.5$. Fixed parameters include $\nu_w = 3 \times 10^{-23}$ cm^3, $\omega = 10^{13}$ s^{-1}, $d = 1$ nm, and $m = 4m_w$. The latter parameters are the masses of trace gas and H_2O molecules. The dependence of $\kappa\lambda$ on P, a, and α_w is rather weak.

[50] The resulting product is shown in Figure 2 as a function of T for selected values of Q given as labels at each curve. The exponential prefactor T^c is a weak function of T with c in the range 0.5–2.5, so that we can expect $\kappa\lambda$ to be essentially dominated by the difference between Q and L. In fact, for $Q \approx L$, there is almost no dependence on T, while $\kappa\lambda$ increases (decreases) moderately for $Q > L$ ($Q < L$). In contrast, there is a marked dependence on Q. The fact that most of the changes occur near $Q = L$ indicates that we deal with physical adsorption phenomena.

[51] As $1/k$ is the time of adsorption (recall section 2.3), kd can be viewed as an escape velocity of molecules due to desorption. Hence the product $\kappa\lambda$ from equation (17) measures the effectiveness of desorption relative to ice growth. The analytical solution derived in section 2.5 shows that $\kappa\lambda$ is the key factor controlling the efficiency of trapping.

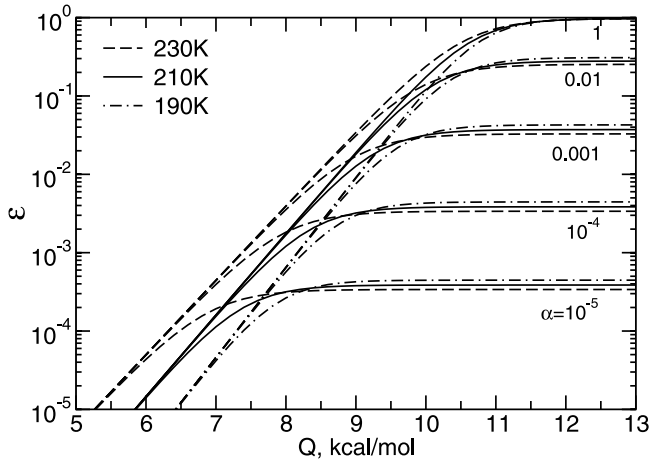

Figure 3. Trapping efficiency ε versus heat of adsorption Q evaluated at various temperatures and deposition coefficients. Other microphysical parameters as in Figure 1. The difference between case $\alpha = 1$ and $\alpha = 0.1$ (not shown) is small.

[52] Decreasing $\kappa\lambda$ causes trapping to become more effective. This can be accomplished, at fixed T, by either decreasing λ via increases of Q, or by increasing $\dot{a}$, that is, the flux of H_2O molecules to the ice particles, via increases of $(S_i - \delta)$.

[53] In Figures 3 and 4 we show the trapping efficiency ε from equation (11) and the uptake coefficient γ from equation (13) as a function of Q for selected values of T and α. The curves represent the limit $\beta\kappa \gg 1$ and exhibit the following general trends.

[54] Both ε and γ take their limiting values β and α, respectively, when Q increases above 8–12 kcal/mol, depending on α, because the time of adsorption increases and more trace gas molecules can become buried. In this regime, uptake of trace gas molecules is only limited by the rate of their gas phase diffusion toward the growing ice particles, or by α. Variations introduced by changing T are rather small, but become important for lower values of Q, where trapping is reduced and the rate at which gases are trapped become sensitive to the ice growth rate and the desorption rate. In this regime, both ε and γ decrease $\propto 1/(\kappa\lambda)$. The exact value of Q for which the transition from adsorption to burial occurs also depends on the choices for a, S_i, and m, besides on α.

[55] The cases with $\beta\kappa \ll 1$ are not achieved for the above choice of parameters. This limit is only approached for extremely low accomodation coefficients; hence equations (15b) and (15d) are hardly encountered in practice.

[56] Figure 5 shows the uptake coefficient as a function of the supersaturation over the ice particle for fixed T and α. The flux of water molecules toward the ice particles is proportional to $(S_i - \delta)$, recall equation (1). We plot γ for selected values of Q. Besides the strong dependence of uptake on Q, Figure 5 shows that trapping is efficient ($\gamma > 10^{-3}$) even at very low supersaturations (<1%), if Q is sufficiently high (>11 kcal/mol).

[57] This is explained by the following estimate. The number of ice monolayers (ML) created by impinging H_2O molecules within a time Δt is given by $\mathrm{ML} = \Delta t \cdot \sigma\dot{a}/\nu_w \sim 1.5\ \Delta t$ [s] at $T = 210$ K, $a = 10$ μm, and $S_i - \delta = 0.01$. Setting $\Delta t = 1/k$ yields $\Delta t \sim 1$ s for $\alpha = 0.1$ and $Q = 11.5$ kcal/mol.

[58] The maximum supersaturations over ice that are observed in cirrus or polar stratospheric cloud conditions are limited by the homogeneous freezing relative humidities of liquid aerosol particles, which typically exceed $S_i = 1.5$. Hence we may expect trapping to be especially effective in the early growth phase of ice particles shortly after freezing.

4. Application

4.1. Numerical Simulations

[59] We apply our results in the microphysical aerosol-cirrus model APSC*m* (Advanced Particle Simulation Code) along atmospheric air parcel trajectories. The version used here calculates aerosol particle growth and evaporation, ice crystal nucleation, growth and sublimation, and trace gas trapping and evaporation from ice particles. The physics of the code has been described in detail elsewhere [*Kärcher*, 2003]. In Appendix C, we briefly describe how equations (10) and (16) are solved numerically in the APSC*m*.

[60] Below we demonstrate how the phase partitioning of a trace gas depends on assumed temperatures and heats of adsorption in idealized cloud scenarios. More realistic scenarios need to incorporate sedimentation of large ice crystals. Such a model set-up would allow to calculate the vertical redistribution of trace gases upon trapping in higher cloud levels and subsequent release from evaporating ice particles at the cloud base. The ice particles in our simulations remain relatively small, for which reason we underestimate the amount of trace gas removal from the gas phase.

[61] Aerosol particles are assumed to consist of aqueous sulfuric acid, which freeze homogeneously at temperatures in the range 3–4 K below the frost point, corresponding to $S_i \geq 1.5$. As we focus on gas-ice interactions, the trace gas is not allowed to dissolve in the liquid particles in the model. The total trace gas volume mixing ratio $\chi = n_\infty \cdot k_B T/P$ is 0.5 ppb, and $P \simeq 200$ mb.

[62] We select 3 heats of adsorption (Q = 8, 11, 14 kcal/mol) to cover the wide range of conditions seen in Figures 3 and 4. We consider a cold case (T = 190–205 K, initialized at $S_i = 1$) and a warm case (T = 215–230 K,

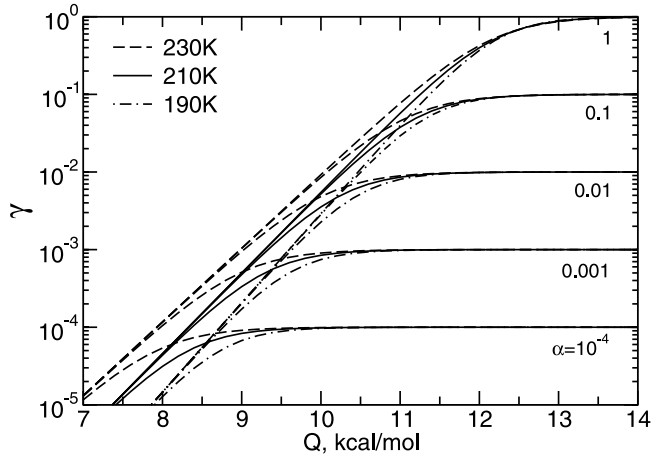

Figure 4. As Figure 3, but for the uptake coefficient γ.

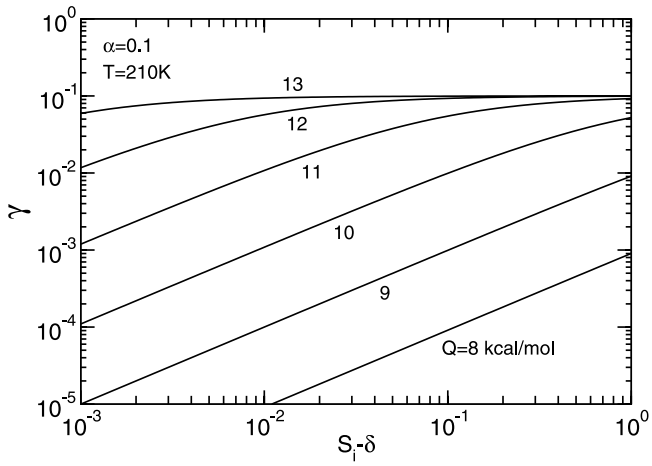

Figure 5. As Figure 4, but now shown as a function of the supersaturation over the ice particle ($S_i - \delta$) evaluated at fixed T and α for selected values of Q.

initialized at $S_i = 1.08$) to mimick tropical/polar and midlatitude conditions, respectively. We use the same mean temperature history ($T(t) - T_b$) for all scenarios taking into account mesoscale temperature fluctuations. The baseline temperature T_b depends on the simulation time t and is defined via $T_0 - (dT/dt) \cdot t$, with a superimposed synoptic cooling rate of $dT/dt = 4.25$ K/d introduced to maintain the clouds after formation and $T_0 = 205$ (230) K in the cold (warm) case.

[63] The curve ($T(t) - T_b$) is shown in Figure 6a over a period of ~2.75 days. It has been created using a simple stochastic model provided by B. Gary (Mesoscale temperature fluctuations: An overview, available at http://reductionism.net.seanic.net/bgary.mtp2/isentrop/index.html, 2002). The resulting ambient ice supersaturation ($S_i - 1$) and ice cloud surface area density $A = \int 4\pi a^2 (dn_i/da) da$ are given in Figures 6b and 6c, respectively, for the cold (blue) and warm (red) case.

[64] The initial mesoscale cooling triggers ice formation after 6 h of simulation time, causing A to increase rapidly. In the cold (warm) case, the cloud persists with up to $A \simeq 10^3$ (10^4) $\mu m^2/cm^3$ until the final warming at $t = 66$ h. Relative to the cold cloud, the warm cloud exhibits a somewhat larger scatter of A and a smaller scatter of S_i, as the H_2O deposition and evaporation rates are faster the higher T. As long as cloud ice exists, S_i oscillates around saturation, causing trace gas molecules being consecutively trapped and released along with H_2O. The amplitudes of these oscillations tend to increase with t because T decreases which in turn causes the timescale for interaction of H_2O molecules with ice particles to increase.

[65] The resulting fraction of trace gas molecules present in the ice phase, ϕ_i, is shown in Figures 6d, 6e, and 6f for $Q = 8$, 10, and 14 kcal/mol, respectively. As expected, fewer molecules partition into the ice phase when Q decreases. One would expect to see higher ϕ_i in the cold cases relative to the warm cases, but this increase is overcompensated by the higher cloud surface area A, see Figure 6c, so that ϕ_i in both cases are comparable most of the time.

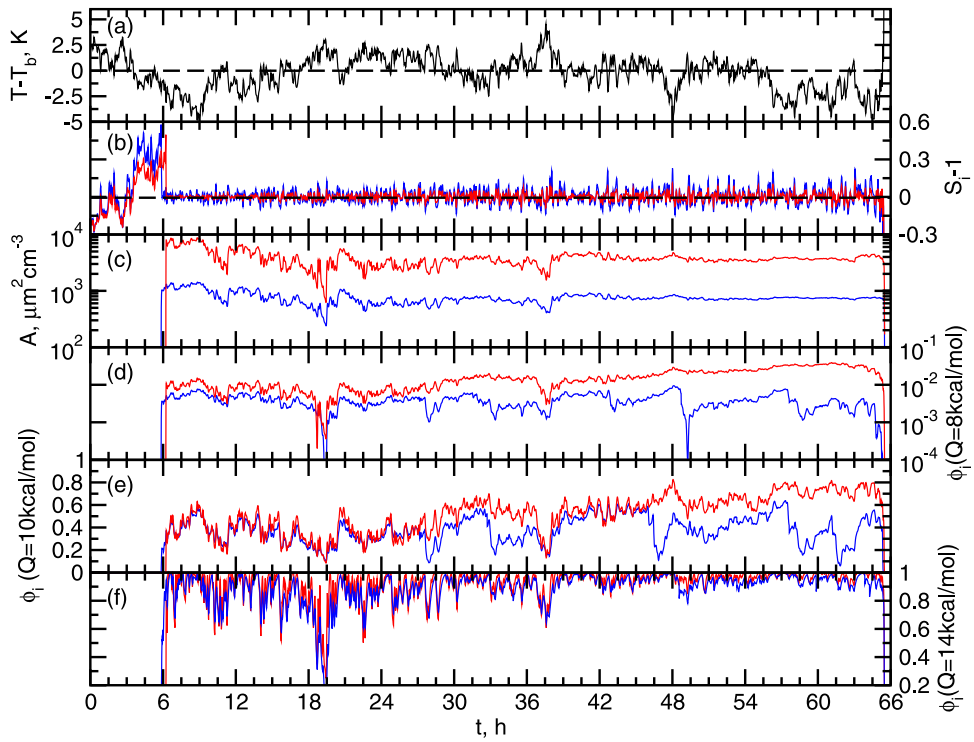

Figure 6. Results of microphysical simulations. Shown are ($T - T_b$) (a) with baseline temperatures $T_b = T_0 - (dT/dt) \cdot t$, and $dT/dt = 4.25$ K/d, $T_0 = 205$ K (blue), and 230 K (red); ambient ice supersaturation ($S_i - 1$) (b); ice cloud surface area density A (c); and ice phase partitioning factor ϕ_i (d), (e), (f) for $Q = 8$, 10, 14 kcal/mol, respectively. In all cases we assume $\alpha = 0.1$. Note the changes in scale in the panels showing ϕ_i.

[66] By Figure 6 we convey three important messages. First, we observe a strong sensitivity of ϕ_i on Q between 8–12 kcal/mol. The ϕ_i-curves also closely follow the variability in supersaturation. Second, most of the trapping occurs in the initial growth phase right after ice nucleation owing to the high supersaturation. Later on, trapping is enhanced in cooling phases, but trace gas molecules frequently evaporate during transient warming phases. Third, although S_i frequently crosses the line $S_i = 1$ at which point $\dot{a} = 0$, fluctuations of S_i drive the ice particles out of equilibrium most of the time, rendering the application of pure adsorption models suspect.

4.2. Relating the Results to HNO_3 Uptake in Cirrus Clouds

[67] Although attempts to model real scenarios and comparisons with observations will be the subject of future work, it is useful to relate the results shown in Figure 6 to the uptake of HNO_3 in ice clouds. This trace gas is present in concentrations ranging from several tens of ppt up to several ppb in the upper troposphere and lower stratosphere.

[68] Most observations report HNO_3 surface coverages (θ), but we find it difficult to compare our results with such data. We argue that ϕ is a better quantity to compare with models. This is because a potentially large and highly variable fraction of HNO_3 may actually reside in the ice particle volume. We agree with *Popp et al.* [2004] that any value of Q inferred (via θ) from gas phase and particulate HNO_3 data taken in the field cannot be regarded as a fundamental thermodynamic parameter unless the data can be corrected for the effect of trapping, e.g., by knowing the history of HNO_3-ice interactions along actual air parcels.

[69] Laboratory measurements suggest that $\alpha \geq 0.3$ [*Hanson*, 1992] and $Q = 10.5 \pm 4$ kcal/mol [*Bartels-Rausch et al.*, 2002] for HNO_3 adsorption on ice. Unfortunately, the experimental uncertainty of ±4 kcal/mol for Q is too large to serve as a robust constraint in uptake models owing to the strong sensitivity of ε and hence ϕ_i near 10 kcal/mol. Future measurements, or more detailed analyses of existing data, may help reduce this uncertainty.

[70] Referring to Figure 6e, and assuming that a value of Q near 10 kcal/mol is appropriate for HNO_3, our model suggests that HNO_3 may be at times present in cloud ice, in accord with field observations in the polar and subtropical tropopause regions [*Kondo et al.*, 2003; *Popp et al.*, 2004]. Less HNO_3 uptake was observed in the upper troposphere at midlatitudes, with lower HNO_3 abundances, lower A, and higher T [*Ziereis et al.*, 2004], again in qualitative agreement with the predictions of our model. More detailed model comparisons to measurements are required to draw a definite conclusion on this point.

5. Discussion of Uncertainties

[71] Our assumption of vanishing diffusion of gases into the ice phase (on the timescales of interest) results in an infinitely thin surface region (recall section 2.4). Most of the uncertainties discussed below are tied to the inability of the model to resolve microphysical processes that occur in the interface between bulk ice and the gas phase.

5.1. Modification of Water Uptake by Adsorbed Molecules

[72] Growth of ice crystals may occur via two-dimensional nucleation at preferred surface sites, such as edges or dislocations [*Hobbs*, 1974]. Molecules adsorbed at the ice surface may block active growth sites for impinging H_2O molecules. This could lead to changes of the crystal habit, growth rate, and size which are not considered in our model. We expect equation (1) to be a good approximation in many practical cases where the number of trace gas molecules present at the ice surfaces is typically smaller than the number of active growth sites.

[73] However, we cannot rule out the possibility that water uptake could be modified, in particular at very low supersaturations. At this point, with the exception of the observations reported by *Gao et al.* [2004], we have no direct evidence that this actually occurs in the atmosphere in cirrus and polar stratospheric cloud conditions. If it occurs, our model can still be applied, but equation (1) has to be replaced by a suitable expression describing the influence of adsorbed gases on dN_w/dt.

5.2. Radial Trace Gas Distribution Within Ice

[74] We assume that trapped molecules become quickly locked within the bulk crystal structure. This should be an excellent approximation in the fast growth (burial) case. In slow growth conditions, foreign molecules might be expelled toward the surface during growth if they do not fit well in the crystal lattice. While this alters the radial distribution of trapped molecules, our model can still be applied to calculate the partitioning of trace gases between the gas and the ice particle phase.

[75] If the molecules expelled to the surface desorb faster than new layers of ice deposit onto the surface, our model will tend to overestimate the amount of molecules in ice. In this limit, however, only few molecules will become trapped, so this uncertainty does not introduce serious errors.

5.3. Limited Adsorption on Ice Crystal Surfaces

[76] Our physical adsorption model allows unlimited uptake and is a good approximation when the number of trace gas molecules is too low to form one or more monolayers at the ice particle surface before the next layers of ice are deposited. This is probably the case for most gases interacting with cirrus or polar stratospheric clouds. Otherwise, the surface may saturate, implying deviations from equation (5). Such deviations may also be brought about by coadsorption of other foreign trace gas molecules.

[77] However, not all gases saturate upon physical adsorption, and surface saturation taking place during particle growth would only be relevant in the adsorption limited cases (15c) and (15d). Besides this, for a given trace gas, it may not always be clear to estimate the exact value σ of the maximum number of available adsorption sites on the surface of an atmospheric ice crystal. Further, it is sometimes difficult to establish the specific functional form of an adsorption isotherm in laboratory uptake experiments. Finally, the effects on γ of uncertainties in determining Q or k (e.g., see section 4.2) can be much more important than the exact knowledge of the specific form of the adsorption isotherm.

[78] Hence we consider surface saturation effects not to be a critical issue for our purpose. A simple estimate under which conditions our model would possibly lead to an overestimation of uptake is as follows. Adsorption may become saturated whenever $n_- = n_+/\lambda \simeq n_\infty/\lambda \geq 1/(\sigma d)$, see section 2.5. Inserting (4) yields

$$k < \frac{\alpha u}{4} \frac{P}{k_B T} \sigma \chi; \tag{18a}$$

evaluating u with $m = 4m_w$ and $T = 215$ K, and using $P = 200$ mbar, $\sigma = 10^{-15}$ cm^2, and $\omega = 10^{13}$ s^{-1}, yields a rough estimate, in practical units,

$$Q\left[\frac{\text{kcal}}{\text{mol}}\right] > \frac{T[\text{K}]}{500} \ln\left(\frac{2 \times 10^{14}}{\chi[\text{ppb}]}\right), \tag{18b}$$

e.g., $Q > 14$ kcal/mol for $\chi = 1$ ppb and $T = 215$ K.

5.4. Kinetic Processes at the Phase Boundary

[79] In section 2.3, we have expressed the rate k in terms of the heat of adsorption and subsequently discussed results in terms of Q. However, owing to the relatively high vapor pressure of ice, the ice surface is highly dynamic even at thermodynamic equilibrium. Typically, 10–1000 monolayers (ML) are exchanged per second at equilibrium between 180–210 K [*Haynes et al.*, 1992]. Therefore, in the limit $\dot{a} = 0$, adsorbed molecules may be affected by the dynamic exchange of H_2O molecules at the ice surface when the time of adsorption $1/k$ exceeds the exchange time τ of ice monolayers, which follows from $\text{ML}/\tau = \sigma(\alpha_w u_w/4)p_i/(k_B T)$, namely,

$$\frac{1}{k} > \frac{\text{ML}}{\sigma} \frac{4}{\alpha_w u_w} \frac{k_{BT}}{p_i}. \tag{19a}$$

Evaluating u_w in (19a) at $T = 215$ K, using $\alpha_w = 0.5$, $\omega = 10^{13}$ s^{-1}, $\sigma = 10^{-15}$ cm^2, and assuming that ML = 5 suffices to modify adsorption compared to a fully static surface yields the rough estimate

$$Q\left[\frac{\text{kcal}}{\text{mol}}\right] > \frac{T[\text{K}]}{500} \ln\left(10^6 \alpha \frac{T[\text{K}]}{p_i[\text{mb}]}\right), \tag{19b}$$

e.g., $Q > 9$ kcal/mol for $\alpha = 0.1$ and $T = 215$ K. Note that this equilibrium consideration must not be confused with cases where $\dot{a} > 0$.

[80] Working with simple adsorption/desorption kinetics may also become inadequate at high temperatures, when the ice surface layer becomes increasingly disordered, or when a surface film forms driven by the presence of solutes, either originating from the gas phase or from scavenging of small aerosol droplets.

[81] Measurements of k will account for the above effects, and in such cases it is favorable to interpret k more generally as an escape rate of the trace gas molecules, i.e., as an effective first order rate that incorporates the above effects. Then, k may still depend on Q, but may depend on other physical parameters describing the overall probability to escape from the dynamic or disordered surface as well.

6. Conclusions

[82] We have presented the first rigorous analytical treatment of the combined effect of mass accomodation and desorption of trace gases on the surfaces of growing ice particles. An approximate solution for the reverse process, the release of trapped trace gases from evaporating ice particles, is also given. The model fully accounts for the dynamic environment in which atmospheric gas-ice interactions are known to take place.

[83] The trapping efficiency and an equivalent nonreactive uptake coefficient are shown to depend on the temperature, ice particle size and radial growth rate, and the gas diffusion coefficient, sticking probability, and rate of desorption of trace gas molecules. Trapping is shown to be controlled by the rate of desorption and the ice growth rate. Trace gases can be effectively trapped in bulk ice even at low ice supersaturations (<1%) when their desorption rates are sufficiently low.

[84] While our model does not resolve all conceivable microphysical processes taking place in a finite surface region separating gas and ice phase, it may still be applied when the desorption rates are interpreted as effective first order escape rates that account for unresolved processes. Cases where gases attached to the ice surface alter the uptake of H_2O molecules may be handled by introducing appropriate ice growth rates.

[85] One way to validate the trapping model is to perform laboratory experiments under controlled, close-to-atmospheric conditions. Alternatively, segments of airborne measurements along Lagrangian flight tracks could be analysed, or existing upper tropospheric data sets could be interpreted by a statistical model analysis.

[86] We have demonstrated, in the context of a microphysical cirrus model, that our approach is useful in carrying out detailed simulations of the atmospheric impact of trapping and will help integrate data from measurements of the phase partitioning with physical theory. It may be possible to combine the uptake coefficient for trapping with reactive uptake coefficients [*Carslaw and Peter*, 1997], permitting to predict the effects of heterogeneous chemical reactions competing with desorption or escape. This possibly provides new insights into the heterogeneous chemistry induced by cirrus or polar stratospheric cloud particles.

[87] The trapping and evaporation equations can easily be implemented in global chemistry-transport models with explicit cloud microphysics and may help improve previous estimates of the chemical effects of vertical redistribution of trace gases trapped in cirrus clouds [*Lawrence and Crutzen*, 1998].

[88] More specifically, our trapping model can be employed to reanalyze the uptake of HNO_3 in cirrus clouds and the resulting denitrification of the upper troposphere. Denitrification is driven by the largest ice crystals which potentially trap HNO_3 most efficiently and sediment to lower altitudes where they release HNO_3 upon evaporation. Previous model studies have considered surface adsorption

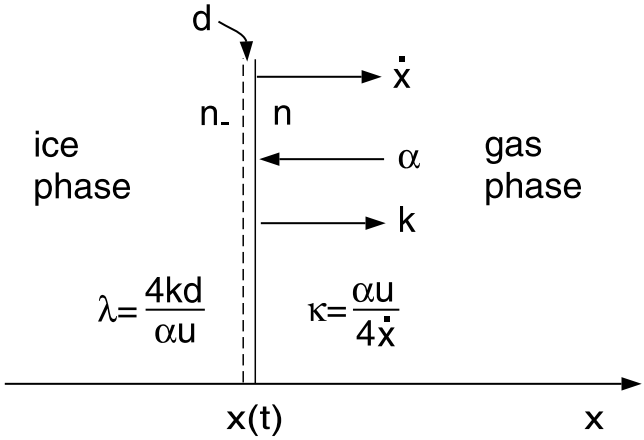

Figure B1. Schematic of processes occurring during trapping of trace gases in growing ice films in planar, free molecular flow.

as the only loss of gaseous HNO_3 and thus likely underestimate the degree of dentrification.

[89] Our model is, of course, not limited to HNO_3-ice interactions. Other atmospherically important species such as hydrogen chloride, hydrogen peroxide, sulfur dioxide, and certain organic vapors can be described as well.

Appendix A: Diffusion in Ice

[90] The steady state flux at $r < a$ is given by

$$f(r) = -n\dot{a} - D_i \frac{dn}{dr} = const. \equiv f_-; \tag{A1}$$

the only solution of equation (A1) that remains finite at $r = 0$ is

$$n(r) = const. \equiv n_- = -f_-/\dot{a}, \tag{A2}$$

irrespective of the value of D_i.

[91] For $\dot{a} = 0$ we get $f_- = 0$, so we essentially have a nonsteady case. The resulting nonsteady flux is given by

$$f_- = -D_i \frac{\partial n}{\partial r}\bigg|_- \simeq -\frac{D_i}{\delta} n_- \simeq -\sqrt{\frac{D_i}{t}} n_-, \tag{A3}$$

where $n_- \simeq n_+/\lambda$ and $\delta \simeq \sqrt{D_i t}$ is the diffusive penetration depth.

[92] The steady state approximation becomes valid when the nonsteady flux component (A3) becomes smaller than its advective counterpart (A2), that is, for

$$t \gg D_i/\dot{a}^2. \tag{A4}$$

As we intend to treat in a time-dependent manner only those processes that occur on timescales $\tau > a/\dot{a}$, identifying t with τ in equation (A4) leads to the required condition

$$D_i \ll a\dot{a}. \tag{A5}$$

Hence the steady state assumption breaks down when $\dot{a} \to 0$. These arguments hold both, in spherical and planar geometry.

[93] As we motivate in section 2.6, a steady state assumption fails when the release of trace gases from evaporating ice particles is considered. Likewise, time-dependent solubility and diffusion in ice must be considered in laboratory uptake experiments with static ice surfaces or on timescales long enough to allow full equilibration between the gas and ice phase [*Dominé and Thibert*, 1996; *Abbatt*, 1997; *Huthwelker et al.*, 2004].

Appendix B: Planar Geometry and Free Molecular Flow

[94] The corresponding processes are sketched in Figure B1. The ice growth rate $\dot{x}$ is related to the flux f_w of H_2O molecules via $\dot{x} = \nu_w f_w$. The supersaturation over the plane ice film is given by $(S_i - 1)$.

[95] In steady state conditions in a coordinate system moving with $\dot{x} > 0$, the trace gas fluxes are given by

$$f_b = -n\dot{x} + (\lambda n_- - n)\frac{\alpha u}{4}, \tag{B1a}$$

$$f_- = -n_-\dot{x}, \tag{B1b}$$

where n is known, because there are no transport limitations in the gas phase. Setting $f_b = f_-$ leads to the following solution for the single unknown n_-,

$$\frac{n_-}{n} = \frac{1+\kappa}{1+\kappa\lambda}, \tag{B2}$$

with κ and λ defined in Figure B1. Note the similarity of equations (B2) and (9). As for the spherical diffusive solution, the factor $\kappa\lambda = kd/\dot{x}$ measures the effectiveness of desorption relative to ice growth, but does not contain the prefactor $(1 - \beta)/\beta$ correcting for gas diffusive transport as noted in equation (17).

[96] The flux into the ice film is $f = n_-\dot{x}$ and the nonreactive uptake coefficient is given by

$$\gamma = \frac{n_-\dot{x}}{nu/4} = \frac{\alpha}{\kappa}\frac{n_-}{n} = \alpha\frac{1+1/\kappa}{1+\kappa\lambda}, \tag{B3}$$

so that $f = n \cdot \gamma u/4$. The following limiting cases are identified.

[97] 1. $\kappa\lambda \ll 1$ (burial limit). Here $\gamma = \alpha$ and $f = n\alpha u/4$ when $\kappa \gg 1$ (gas kinetic burial) and $\gamma = \alpha/\kappa$ and $f = n\dot{x}$ when $\kappa \ll 1$ (ice-growth dominated burial).

[98] 2. $\kappa\lambda \gg 1$ (adsorption limit). Here $\gamma = \alpha/(\kappa\lambda)$ and $f = n\alpha u/4 \cdot \dot{x}/(kd)$ when $\kappa \gg 1$ and $\gamma = \alpha/(\kappa^2\lambda)$ and $f = n\dot{x} \cdot \dot{x}/(kd)$ when $\kappa \ll 1$. Similar to the spherical case, the limiting cases comprise dependences $dN/dt \propto (dN_w/dt)^c$, with $c = 0 \cdots 2$.

[99] When finalizing this manuscript, we learned about laboratory experiments demonstrating enhanced uptake of hydrogen chloride by growing ice films [*Abbatt et al.*, 1992; T. Huthwelker, personal communication, 2004]. A model similar to equation (B3) has been independently developed

and applied to the latter measurements. A preliminary data analysis indicates that the same processes described in our paper have caused gas trapping in these experiments. This increases confidence that the trapping concept is capable of providing consistent interpretations of laboratory uptake experiments [*Huthwelker*, 1999], besides simulating related processes occurring in the atmosphere.

Appendix C: Numerical Solution

[100] The flux equation (11) involves no loss term for N. In the APSC*m*, it is solved along with the conservation of the total trace gas mixing ratio in the air parcel by applying the analytical predictor for condensation scheme as introduced by *Jacobson* [1999].

[101] To solve equation (16), again ensuring mass balance between the gas and ice phase, we use the analytical predictor for dissolution scheme [*Jacobson*, 1999], as dN/dt involves only a loss term $\propto N$. More specifically, we introduce a pseudo-Henry's law constant H by casting equation (16) into the form

$$\frac{dN}{dt} = -4\pi a D_w \beta_w \frac{N}{H}, \quad H = \frac{N_w \cdot k_B T / p_i}{|S_i - \delta|}. \tag{C1}$$

This approach, albeit approximate, is physically reasonable as $dN/dt \propto \dot{a}$.

[102] The equation describing the depletion of the trace gas from its gas phase reservoir reads

$$\frac{dn_\infty}{dt} = -\int_0^\infty \frac{dN}{dt}\frac{dn_i}{da}da, \tag{C2}$$

with the ice crystal size distribution dn_i/da.

Notation

a ice particle radius.
$\dot{a}$ ice particle growth rate.
d ice surface depth.
f total molecular flux.
k rate of desorption.
k_B Boltzmann constant.
m molecular mass.
n number density in a given phase.
p partial pressure or saturation vapor pressure.
r radius variable.
t time.
u mean thermal speed of molecules.
$\dot{x}$ ice growth rate in planar flow.
A ice cloud surface area density.
D diffusion coefficient.
H pseudo-Henry's law constant.
K equilibrium constant for adsorption.
N number of molecules per ice particle.
P air pressure.
Q heat of adsorption.
S saturation ratio.
T air temperature.
α accomodation coefficient.
β correction factor for gas phase diffusion.
γ uptake coefficient.
δ Kelvin barrier.
ε trapping efficiency.
θ fractional ice surface coverage.
κ dimensionless timescale parameter.
λ dimensionless adsorption parameter.
μ molar ratio between trace gas and H_2O in ice.
ν volume of molecules in ice.
σ area of one adsorption site.
ϕ fraction of molecules in a given phase.
χ gas volume mixing ratio.
ω oscillation frequency of molecules.

Subscripts

i ice phase.
w water, H_2O.
$+$ gas phase at $r \searrow a$.
$-$ ice phase at $r \nearrow a$.
∞ gas phase at $r \gg a$.

[103] **Acknowledgments.** Much of this work was motivated while B.K. stayed at NOAA's Aeronomy Laboratory in Boulder, Colorado. He is grateful to David Fahey, Ru-Shan Gao, and Peter Popp for fruitful discussions. We also appreciate stimulating discussions with Thomas Huthwelker, who provided us with a manuscript describing related laboratory studies prior to publication. This work was funded, in part, by the European Commission within the Integrated Project "Stratosphere-Climate Links With Emphasis on the UTLS" (SCOUT-O3), and by the DLR/HGF-project "Particles and Cirrus Clouds" (PAZI-2).

References

Abbatt, J. P. D. (1997), Interaction of HNO_3 with water-ice surfaces at temperatures of the free troposphere, *Geophys. Res. Lett.*, *24*, 1479–1482.

Abbatt, J. P. D., K. D. Beyer, A. F. Fucaloro, J. R. McMahon, P. J. Woolridge, R. Zhang, and M. J. Molina (1992), Interaction of HCl vapor with water-ice: Implications for the stratosphere, *J. Geophys. Res.*, *97*, 15,819–15,826.

Bartels-Rausch, T., et al. (2002), The adsorption enthalpy of nitrogen oxides on crystalline ice, *Atmos. Chem. Phys.*, *2*, 235–247.

Carslaw, K. S., and T. Peter (1997), Uncertainties in reactive uptake coefficients for solid stratospheric particles: 1. Surface chemistry, *Geophys. Res. Lett.*, *24*, 1743–1746.

Crank, J. (1956), *The Mathematics of Diffusion*, Oxford Univ. Press, New York.

de Boer, J. H. (1968), *The Dynamical Character of Adsorption*, Oxford Univ. Press, New York.

Dominé, F., and E. Thibert (1996), Mechanism of incorporation of trace gases in ice grown from the gas phase, *Geophys. Res. Lett.*, *23*, 3627–3630.

Gao, R.-S., et al. (2004), Evidence that nitric acid increases relative humidity in cirrus clouds, *Science*, *303*, 516–520.

Hanson, D. R. (1992), The uptake of HNO_3 onto ice, NAT, and frozen sulfuric acid, *Geophys. Res. Lett.*, *19*, 2063–2066.

Haynes, D. R., N. J. Tro, and S. M. George (1992), Condensation and evaporation of H_2O on ice surfaces, *J. Phys. Chem.*, *96*, 8502–8509.

Hobbs, P. V. (1974), *Ice Physics*, Clarendon, Oxford, UK.

Huthwelker, T. (1999), Experimente und Modellierung der Spurengasaufnahme in Eis, Ph.D. dissertation, Univ. Bonn, Bonn, Germany.

Huthwelker, T., M. E. Malmström, F. Helleis, G. K. Moortgat, and T. Peter (2004), Kinetics of HCl uptake on ice at 190 and 203 K: Implications for the microphysics of the uptake process, *J. Phys. Chem. A*, *108*, 6302–6318.

Jacobson, M. Z. (1999), *Fundamentals of Atmospheric Modeling*, Cambridge Univ. Press, New York.

Kärcher, B. (2003), Simulating gas-aerosol-cirrus interactions: Process-oriented microphysical model and applications, *Atmos. Chem. Phys.*, *3*, 1645–1664.

Kondo, Y., et al. (2003), Uptake of reactive nitrogen on cirrus cloud particles in the upper troposphere and lowermost stratosphere, *Geophys. Res. Lett.*, *30*(4), 1154, doi:10.1029/2002GL016539.

Lawrence, M. G., and P. J. Crutzen (1998), The impact of cloud particle gravitational settling on soluble trace gas distributions, *Tellus, Ser. B*, *50*, 263–289.

Legrand, M. (1994), Ice core chemistry: Implications for our past atmosphere, in *Low Temperature Chemistry of the Atmosphere*, *NATO ASI*

Ser. I, vol. 21, edited by G. K. Moortgat et al., pp. 421–445, Springer-Verlag, New York.

Marti, J., and K. Mauersberger (1993), A survey and new measurements of ice vapor pressure at temperatures between 170 and 250 K, *Geophys. Res. Lett.*, *20*, 363–366.

Popp, P. J., et al. (2004), Nitric acid uptake on subtropical cirrus cloud particles, *J. Geophys. Res.*, *109*, D06302, doi:10.1029/2003JD004255.

Pruppacher, H. R., and J. D. Klett (1997), *Microphysics of Clouds and Precipitation*, Kluwer Acad., Norwell, Mass.

Tabazadeh, A., O. B. Toon, and E. J. Jensen (1999), A surface chemistry model for nonreactive trace gas adsorption on ice: Implications for nitric acid scavenging by cirrus, *Geophys. Res. Lett.*, *26*, 2211–2214.

World Meteorological Organization (WMO) (2003), Scientific assessment of ozone depletion, *Rep. 47*, Global Ozone Res. and Monit. Proj., Geneva.

Yin, Y., K. S. Carslaw, and D. J. Parker (2002), Redistribution of trace gases by convective clouds—Mixed-phase processes, *Atmos. Chem. Phys.*, *2*, 293–306.

Ziereis, H., et al. (2004), Uptake of reactive nitrogen on cirrus cloud particles during INCA, *Geophys. Res. Lett.*, *31*, L05115, doi:10.1029/2003GL018794.

M. M. Basko, Institute for Theoretical and Experimental Physics, B. Cheremushkinskaya 25, 117218 Moscow, Russia.

B. Kärcher, Institut für Physik der Atmosphäre, Deutsches Zentrum für Luft- und Raumfahrt, 82234 Wessling, Germany. (bernd.kaercher@dlr.de)